Journal of Solid State Chemistry **152,** 105–112 (2000)
doi:10.1006/jssc.2000.8705, available online at http://www.idealibrary.com on IDEAL®

Novel Extended Solids Composed of Transition Metal Oxide Clusters

M. Ishaque Khan

Department of Biological, Chemical, and Physical Sciences, Illinois Institute of Technology Chicago, Illinois 60616

Transition metal oxide clusters and their derivatives offer an unmatched variety of structural motifs that are potential building blocks for the design and development of extended solids. In view of the proven applications of these clusters in catalysis, molecular recognition, environmental decontamination, clinical and analytical processes, materials science, nanotechnology, and medicine, their usage as building blocks promises the development of new materials whose properties could be rationalized in terms of their constituents. Although the technique of assembling appropriate transition metal oxide clusters to generate new solids is still underdeveloped, recent progress made in this direction is promising. During our ongoing research program focused on this aspect, we have been able to prepare and characterize a series of novel framework materials, composed of well defined vanadium oxide clusters $\{V_{18}O_{42}(XO_4)\}$ (X = V, S, Cl). We have also prepared three-dimensional composite solids by incorporating organic ligands into the transition metal oxide framework. Some of the results of this work are reviewed with reference to the synthesis, structure, and physicochemical properties of the newly prepared extended solids. © 2000 Academic Press

Key Words: **crystal structure; framework solids; metal oxides; mixed-valent compounds; polyoxometalates; poloxovanadates; ion exchange; thermogravimetry; composite materials; hybrid solids.**

1. INTRODUCTION

Transition metal oxide clusters, or polyoxometalates (1), represent an expanding class of molecular systems with wide ranging applications in several areas such as analytical chemistry, materials science and catalysis, nanotechnology, chemical sensing, environmental decontamination, biochemical and geochemical processes, and medicine (1d, 2, 3). These fascinating metal oxide aggregates may contain up to hundreds of metal atoms fused together via oxide ligands which may be present in various (μ_2, μ_3, μ_4, μ_6, etc.) bridging modes. Remarkably, they remain unsurpassed in providing a wide variety of robust structural motifs of different topologies and sizes which could be connected in several different ways (1e).

Polyoxovanadates, or vanadium oxide clusters (1a–1c), constitute an important but, as compared to polyoxomolybdates and polyoxotungstates, relatively less studied subclass of polyoxometalates. A number of polyvanadates containing 3 to as many as 34 vanadium atoms with interesting physicochemical properties have been synthesized and characterized in recent years (1c, 4, 5). Most of the clusters of higher nuclearity (e.g., $[V_{12}O_{32}]^{4-}$ (6a), $[V_{15}O_{36}]^{5-}$ (6b), $[V_{18}O_{42}]^{12-}$ (7), $[V_{19}O_{49}]^{9-}$ (8), and $[V_{34}O_{82}]^{10-}$ (9)) may formally be regarded as vanadium-oxide shells that may be assembled around a variety of encapsulated species (10) that appear to exert templating effects in determining the shapes and sizes of the shells surrounding them. These clusters may contain fully oxidized, reduced, or mixed-valence vanadium centers. Due to the extensive magnetochemistry associated with the reduced and mixed-valence systems, there has been a growing interest in, systematically, increasing the size of these clusters (5). Besides their possible implications in the development of chemical systems with potential use in preparing new (magnetic and electronic) devices (11), these systems may also make it possible to explore the limit of the miniaturization of magnets.

Most of the known polyoxometalates are generally stable in air at room and even at elevated temperatures and they could be inexpensively and efficiently prepared in conventional synthetic laboratories. Given the increasingly larger and impressive array of the robust structural motifs provided by the polyoxometalates and their proven applications in several areas of contemporary interest (1d), it will be valuable to develop strategies involving the use of well characterizable oxometalate motifs for the design and development of new materials. Progress in this direction may pave the way for the rational synthesis of transition metal oxide based materials, containing well characterizable motifs with desired features, whose properties could readily be modified and possibly rationalized in terms of their constituents at the molecular levels. Fashioning materials with controllable properties to meet the environmental and technological challenges of modern times is an emergent theme of contemporary research.

However, the technique of bringing suitable transition metal oxide motifs to generate new metal oxide-based

0022-4596/00 $35.00

materials with desirable properties is still in its infancy. We have an ongoing program focused on the design and development new extended solids composed of well characterized transition metal oxide clusters. At the beginning of this work, the assembling of polyoxometalate clusters has been limited to the preparation of mainly few one-dimensional materials (12). In this article we will describe a series of novel framework solids which we have recently synthesized and characterized (13–18). Although there are some fragmentary reports on solids derived from polyoxomolybdates and polyoxotungstates (12a–12e) the present discussion is focused on the materials which are composed of polyoxovanadate motifs.

2. SYNTHESIS OF EXTENDED SOLIDS COMPOSED OF $\{V_{18}O_{42}\}$ CLUSTERS

The $\{V_{18}O_{42}\}$ core has been observed in a number of well characterized compounds containing varying numbers of reduced vanadium(IV) sites (7, 13–18). The structure of $\{V_{18}O_{42}\}$ and several other V/O shells found in recently prepared clusters are derived from the appropriate fragments of the vanadium pentaoxide sheets (4). The basic $\{V_{18}O_{42}\}$ shell in all these compounds is constructed from $18\{VO_5\}$ square pyramids sharing edges through 24 μ_3-oxygen atoms. The shell could incorporate VO_4^{3-} and SO_4^{2-} (7a, 13, 14) and encapsulate a variety of anions (Cl^-, Br^-, I^-, NO_2^-, SH^-, S^{2-}, $HCOO^-$) and neutral molecules of appropriate sizes (7a). We have prepared and characterized a series of novel framework materials composed of well defined $\{V_{18}O_{42}(XO_4)\}$ (X = S, V, Cl) building blocks (13–18).

The $\{V_{18}O_{42}(XO_4)\}$ (X = V, S, Cl, OH, etc.) species could readily be generated in aqueous solutions which may directly be used for reactions with a number of other metal salts to prepare a variety of materials with extended structures. Thus, the reaction of hot (80–95°C) aqueous solution of the MVO_3 (M = Li, Na, K, or NH_4), obtained from the reaction of the aqueous slurry of V_2O_5 with MOH, with common reducing agents (e.g., hydrazinium sulfate, hydrazinium chloride, or Zn metal), results in a deep colored solution (pH ~ 4.6). The solution reacts with a variety of metal salts, such as $MnCl_2 \cdot 4H_2O$, $KMnO_4$, $FeCl_2 \cdot 4H_2O$, $CoSO_4 \cdot 6H_2O$, $NiSO_4 \cdot 6H_2O$, $CdSO_4 \cdot 8H_2O$, and $MgSO_4 \cdot 7H_2O$, to give novel framework materials (13–16, 18). This general method has been employed by us to prepare a series of novel three-dimensional solids with extended structures composed of well defined vanadium oxide clusters $\{V_{18}O_{42}(XO_4)\}$. The newly prepared class of materials is described below with the help of the following representative examples:

$[Mn^{II}_3(H_2O)_{12}H_6V^{IV}_{15}V^{V}_3O_{42}(V^{V}O_4)] \cdot 30H_2O$ (**1**)

$Li_6[Fe^{II}_3(H_2O)_{12}V^{IV}_{15}V^{V}_3O_{42}(V^{V}O_4)] \cdot 24H_2O$ (**2**)

$Li_6[Ni^{II}_3(H_2O)_{12}V^{IV}_{16}V^{V}_2O_{42}(SO_4)] \cdot 24H_2O$ (**3**)

$(N_2H_5)_2[Zn^{II}_3(H_2O)_{12}V^{IV}_{12}V^{V}_6O_{42}(SO_4)] \cdot 24H_2O$ (**4**)

$[M^{II}_3(H_2O)_{12}V_{18}O_{42}(XO_4)] \cdot 24H_2O$
(M = Fe, **5**; M = Co, **6**; X = V, S)

$Li_6[Cd^{II}_3(H_2O)_{12}V_{18}O_{42}(XO_4)] \cdot 24H_2O$ (X = V, S) (**7**)

$Li_6[Mn^{II}_3(H_2O)_{12}V^{IV}_{16}V^{V}_2O_{42}(XO_4)] \cdot 24H_2O$ (X = V, S) (**8**)

The compounds were characterized by elemental and thermogravimetric analyses, spectroscopic methods, manganometric titration, ion exchange, X-ray diffraction, and complete single crystal structure analyses.

The mixed-metal compound $[Mn_3(H_2O)_{12}V_{18}H_6O_{42}(VO_4)] \cdot 30H_2O$ (**1**) could be obtained in high yield by the reaction of $KMnO_4$ with the dark colored solution which is obtained by treating with hydrazinium sulfate the solution that results from the reaction of aqueous solution of $LiOH \cdot H_2O$ with a slurry of V_2O_5 in water at 95°C. Although **1** could be prepared over a wide range of different reaction temperatures and slightly different reaction stoichiometries and reactants, the optimum reaction temperature is ~95°C. The reactions leading to the formation of **1** are, however, pH sensitive. The reactions carried out in neutral and basic media did not yield **1**, giving intractable orange brown amorphous materials. The reactions using $MnCl_2$ or $MnSO_4$ in place of $KMnO_4$ yielded a slightly different compound $Li_6[Mn^{II}_3(H_2O)_{12}V^{IV}_{16}V^{V}_2O_{42}(XO_4)] \cdot 24H_2O$ (X = V, S) (**8**) which crystallized in a different space group with more regular structure than what is observed in **1** (see below). Using iron(III) chloride in place of $KMnO_4$ resulted into the formation of $Li_6[Fe^{II}_3(H_2O)_{12}V_{18}O_{42}(VO_4)] \cdot 24H_2O$ (**2**) (18).

The reaction of aqueous solution of lithium vanadate with hydrazinium sulfate results into a dark colored solution which reacts with nickel(II) sulfate hexahydrate and zinc(II) sulfate heptahydrate to yield dark greenish-black prism shaped crystals of $Li_6[Ni^{II}_3(H_2O)_{12}V_{18}O_{42}(SO_4)] \cdot 24H_2O$ (**3**) and $(N_2H_5)_2[Zn^{II}_3(H_2O)_{12}V_{18}O_{42}(SO_4)] \cdot 24H_2O$ (**4**), respectively. The presence of sulfate ion in the reaction mixture is essential for the syntheses of **3** and **4**. Thus, while it can also be prepared by using hydrazine chloride ($NH_2NH_2 \cdot 2HCl$) in place of hydrazine sulfate or by substituting nickel sulfate with nickel chloride in the above described synthetic method, **3** could not be synthesized when both sulfate sources ($NiSO_4 \cdot 6H_2O$ and $NH_2NH_2 \cdot SO_4$) were replaced by $NiCl_2 \cdot 6H_2O$ and $NH_2NH_2 \cdot 2HCl$, respectively; instead, in the latter case, a brown-black powder of a different material was obtained, which was not further characterized.

Prism shaped crystals of $[M^{II}_3(H_2O)_{12}V_{18}O_{42}(XO_4)] \cdot 24H_2O$ (M = Fe, **5**; M = Co, **6**; X = V, S) could be isolated from the dark colored solution obtained from the reaction of V_2O_5 with $LiOH \cdot H_2O$, hydrazinium sulfate

and $FeCl_2 \cdot 4H_2O$ or $CoSO_4 \cdot 6H_2O$ in water at 84–86°C. The analogous reactions yield the greenish-black species $Li_6[Cd_3(H_2O)_{12}V_{18}O_{42}(XO_4)] \cdot 24H_2O$ (**7**) and $Li_6[Mn^{II}_3(H_2O)_{12}V_{18}O_{42}(XO_4)] \cdot 24H_2O$ ($X = V$, S) (**8**) when, respectively, $CdSO_4 \cdot 8H_2O$ and $MnCl_2 \cdot 4H_2O$ or $MnSO_4$ are allowed to react with the reduced polyvanadate solution.

3. PHYSICAL AND SPECTRAL PROPERTIES

All these compounds were isolated in highly crystalline forms. The crystals of the materials exhibit shining faces and deep colors characteristic of the reduced and mixed-valence compounds. The number of reduced vanadium(V^{IV}) centers per formula unit in each compound was determined by the manganometric titration of the acidic solution of the corresponding compound against standardized $KMnO_4$ solution.

These materials are, generally, stable in air and are insoluble in common solvents. For example, crystals of **1** are indefinitely stable in air, insoluble in cold water and common organic solvents, slightly soluble in warm water, moderately soluble in DMSO giving purple-black colored solution which is stable for several days at room temperature, and quite soluble in boiling water. The aqueous solution of **1** changed color from black to light green to yellow within few hours. When stored under nitrogen, most of these solids are indefinitely stable. Crystals of **3** undergo slow deterioration, losing their shining faces, which slowly develop cracks at room temperature. This, however, could be minimized when the reaction temperature and/or reaction time for preparing **3** is somewhat increased. Some of the crystals, notably those of **3**, **5**, and **7**, undergo slow oxidation in air. Consequently, the number of reduced (V^{IV}) sites decreases with time.

The infrared absorption spectra of these compounds exhibit vibrational bands due to the functionalities associated with $\{V_{18}O_{42}(XO_4)\}$ core and coordinated and lattice water molecules. The strong bands in the 1000–900 cm^{-1} region are characteristic of $\upsilon(V{=}O)$ modes. Multiple features attributable to the bridging V–O–V groups are found in the 840–400 cm^{-1} region.

4. STRUCTURAL PROPERTIES

The single crystal structure analyses of the compounds described in the foregoing paragraphs revealed extended and highly symmetrical three-dimensional framework structures which are closely related.

The extended structure of the crystals of **1**, shown in Fig. 1, is composed of the transition metal oxide building-block units given in Fig. 2. The structure consists of $\{V_{18}O_{42}(VO_4)\}$ clusters each one of which is linked by six $\{Mn(H_2O)_4\}$ bridges to six other neighboring

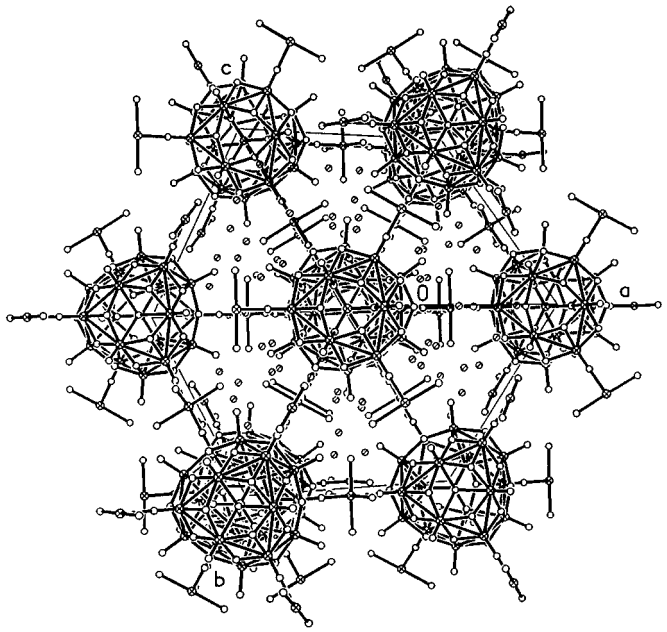

FIG. 1. A view of the structure of $[Mn_3(H_2O)_{12}V_{18}H_6O_{42}(VO_4)] \cdot 30H_2O$ (**1**) showing arrays of $\{V_{18}O_{42}(VO_4)\}$ "spheres" interconnected through $\{Mn(H_2O)_4\}$ bridging groups and channels occupied by the water molecules (striped circles) of crystallization. Hydrogen atoms are not shown.

$\{V_{18}O_{42}(VO_4)\}$ units generating a three-dimensional network of $[-\{V_{18}O_{42}(VO_4)\}-\mu_2-Mn(H_2O)_4-\{V_{18}O_{42}(VO_4)\}-]_\infty$ arrays. The constituent $\{V_{18}O_{42}(VO_4)\}$ cluster is constructed from the $\{V_{18}O_{42}\}$ shell encapsulating a tetrahedral $\{VO_4\}^{3-}$ group which interacts with the 12-V centers of the shell, each oxygen of the $\{VO_4\}^{3-}$ unit (V–O = 1.661 Å) interacting in μ_4 mode with three V centers, forming $V(1)–O(1)–V(2)_{shell}$ bonds ($O1–V_{shell}$ = 2.440 Å) and forcing the local idealized tetrahedral symmetry upon the $\{V_{18}O_{42}(VO_4)\}$ unit.

The $\{V_{18}O_{42}\}$ shell is known for exhibiting molecular container property. The shell may exist with different electronic populations in two closely related structural forms with different symmetries (T_d and D_{4d}) which are influenced by the stereochemical needs and the extent of interaction of the encapsulated moiety—the "guest species"—with the V centers of the shell (7a, 14). For example, in the $Na_6[H_7V^{IV}_{16}V^{V}_{2}O_{42}(VO_4)] \cdot 21H_2O$ cluster (7a), the $\{VO_4\}^{3-}$ (V–O = 1.71 Å) group interacts through 4 $\{\mu_4–O\}$ with the 12-V centers of the shell forming covalent $(V–\mu_4–O)–V_{shell}$ ($\mu_4–O–V_{shell}$ = 2.39 Å) bonds and conferring the tetrahedral symmetry to the cluster anion similar to what is observed in **1**.

The $12\{VO_6\}$ units of $\{V_{18}O_{42}(VO_4)\}$ core in **1** (14) are fused with $6\{VO_5\}$ groups through common edges and linked with the central $\{VO_4\}$ unit via corner sharing. The

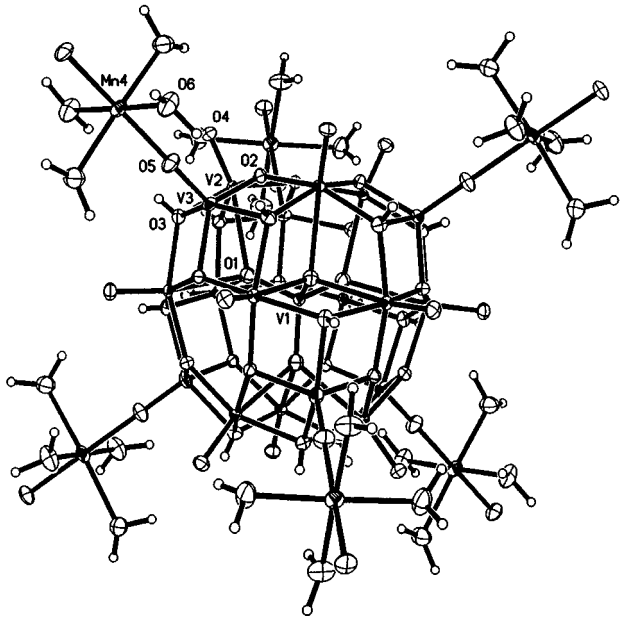

FIG. 2. The building block units in the crystal structure of $[Mn_3(H_2O)_{12}V_{18}H_6O_{42}(VO_4)]\cdot 30H_2O$ (**1**) showing the atom labeling scheme in the asymmetric unit. Small open circles represent hydrogen atoms.

octahedral geometry around each vanadium in the $12\{VO_6\}$ units is defined by a terminal oxo-group (V–O = 1.609 Å), four μ_3-oxygens of the shell (V–O = 1.949–1.981 Å), and one μ_4-oxygen (O–V = 2.440 Å) from the central $\{VO_4\}$ unit. The geometry around each one of the square-pyramidal V(3) in $6\{VO_5\}$ is defined by four basal μ_3-oxo groups (V–O = 1.889–2.019 Å) from the shell and an apical μ_2-oxygen (O(5)) (V–O = 1.640 Å) that, in turn, is linearly bonded to the manganese(II) center of one of the six $\{Mn(H_2O)_4\}$ bridges, forming $\{V–O–Mn–O(5)–V\}$ bonds, responsible for interlinking $\{V_{18}O_{42}(VO_4)\}$ clusters. The octahedral geometry around each manganese(II) is completed by four oxygen atoms from the aqua ligands (Mn–O(H_2) = 2.200 Å), each one disordered over three positions, and two *trans*-μ_2-oxo groups (O(5)) (Mn–O = 2.136 Å). The framework structure in **2** is essentially isomorphous to that observed in **1** with the exception that the constituent $\{V_{18}O_{42}(VO_4)\}$ clusters in **2** are interconnected by $\{Fe(H_2O)_4\}$ bridging groups.

The crystal structures of **3** (18) and **4** (13) (Fig. 3) consist of arrays of $\{V_{18}O_{42}(SO_4)\}$ clusters, each one connected to six others via $\{Ni(H_2O)_4\}$ and $\{Zn(H_2O)_4\}$ bridging groups, respectively. The building block units in the structure of **4**, shown in Fig. 4, consist of $\{V_{18}O_{42}(SO_4)\}$ cluster formed from the $\{V_{18}O_{42}\}$ shell hosting a tetrahedral $\{SO_4\}^{2-}$ moiety with disordered oxygen atoms. The guest $\{SO_4\}^{2-}$ group, unlike the encapsulated $\{VO_4\}^{3-}$ groups in **1** and **2**, is not an integral part of the shell and has normal S–O distances (1.472 Å).

Figure 5 represents the isomorphous structures of the mixed-valence compounds **5–8** (15, 18). The structures of these materials consist of $\{V_{18}O_{42}\}$ cages with crystallographic $m\bar{3}m$ (O_h) symmetry (19) linked by bridging $\{M(H_2O)_4\}$ groups (M = Fe, Co, Cd, Mn) into two interpenetrating three-dimensional networks—a consequence of body-centered symmetry (20). Each cage hosts a twofold disordered tetrahedral $\{XO_4\}$ group. Based on crystallographic, chemical, and spectroscopic evidence (21), the final refinement model assumed a disordered distribution of both (VO_4^{3-} and SO_4^{2-}) anions for the $\{XO_4\}$ group. A view of the $[V_{18}O_{42}(XO_4)]$ cluster in **5** is shown in Fig. 6. All bond distances in the cluster are within normal ranges. The geometry around V(1) centers in $12\{VO_5\}$ groups is defined by a terminal oxo-(O(2)) group and four μ_3–O(1) atoms. The geometry around V(2) in the remaining $6\{VO_5\}$ units is defined by four μ_3-O(1) groups and an apical μ_2–O(3), which is also bonded to the M^{II} center of one of the six $\{M(H_2O)_4\}$ bridges that interlink $\{V_{18}O_{42}(XO_4)\}$ clusters. The coordination sphere of M^{II} is completed by the four oxygen atoms from the aqua ligands (M–O(H_2) = 2.089 Å for **5** and 2.047 Å for **6**), each one exhibiting a twofold disorder, and two *trans*-μ_2–O(3) groups. The elongated ellipsoid for O(1), present in **5–6**, is probably a consequence of steric interactions arising from a short O ··· O contact

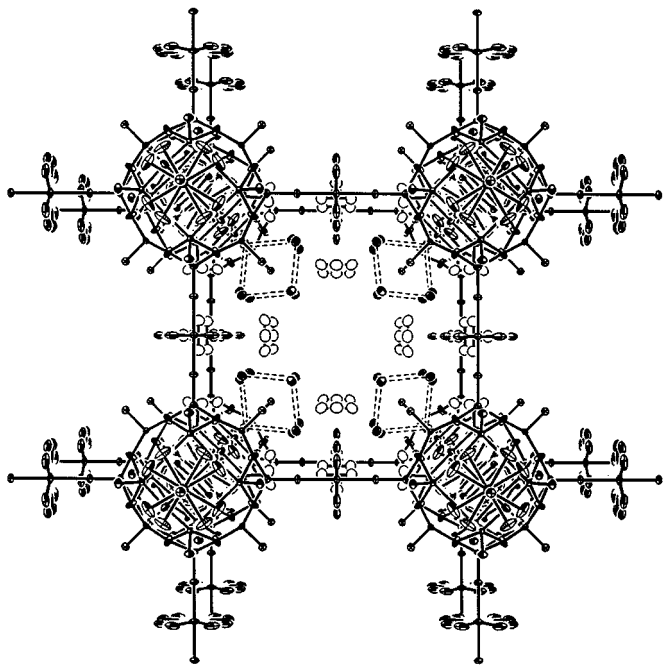

FIG. 3. View of the extended structure of $(N_2H_5)_2[Zn_3(H_2O)_{12}V_{18}O_{42}(SO_4)]\cdot 24H_2O$ (**4**) showing interpenetrating nets of $\{V_{18}O_{42}(SO_4)\}$ clusters interconnected through $\{Zn(H_2O)_4\}$ bridging groups, and rectangular channels occupied by the hydrogen bonded water molecules (open circles) and cations (striped circles). Hydrogen atoms and the central cluster in the unit cell have been omitted.

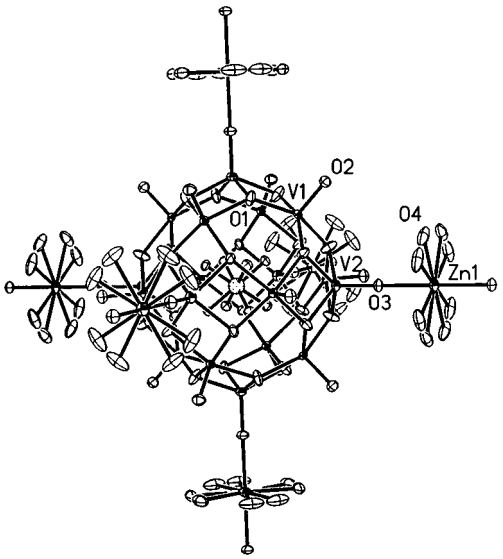

FIG. 4. The building block units in the crystal structure of $(N_2H_5)_2[Zn_3(H_2O)_{12}V_{18}O_{42}(SO_4)]\cdot 24H_2O$ (**4**) showing the atom labeling scheme. The stippled central circle represents a sulfur atom; atoms bonded to the sulfur atom represent O5 atoms. Selected bond lengths: **4**, V(1)–O(2) = 1.588 Å; V(1)–O(1) = 1.9515 Å; V(2)–O(3) = 1.634 Å; V(2)–O(1) = 1.953 Å; Zn(1)–O(4)(H_2) = 2.063 Å; Zn(1)–O(3) = 2.122 Å; S(1)–O(5) = 1.472 Å; V(1)–V(2) = 2.9441 Å.

(2.545(9) Å for **5** and 2.521(13) Å for **6**) between O(1) and an O(4) site that is only 50% occupied.

The M–O distances and bond valence sum (BVS) (22) values ($\sim$0.35) of the four oxygen atoms present in the bridging $\{M(H_2O)_4\}$ groups in **1–8** clearly identify these oxygens as H_2O. This conclusion and the results of the manganometric titration of V^{IV} sites are consistent with the charge balance consideration and the above formulations of **1–8**.

The extended structures in **1–8** contain cavities that are occupied by counterions and/or lattice water molecules. The lattice water in the cavities are hydrogen bonded to the oxo-groups present on the surface of the $\{V_{18}O_{42}(XO_4)\}$ clusters. Moreover, the lattice water molecules are clustered together through intermolecular hydrogen bonds. A view of such clusters present, as $\{(H_2O)_6\}$ groups, in the cavities of $Li_6[Cd_3(H_2O)_{12}V_{18}O_{42}(XO_4)]\cdot 24H_2O$ (**7**) is shown in Fig. 7.

5. THERMAL AND ION EXCHANGE PROPERTIES

The lattice water occupying the voids present in the above-described materials is readily removable at relatively lower temperatures. The thermogravimetric analysis of a sample of **1** shows initial weight loss corresponding to the total removal of the lattice water at 70°C followed by the weight loss due to the removal of coordinated water at $\sim$257°C. Further heating up to 500°C yielded a reduced metal oxide phase. The dehydrated (at 120°C) sample of **1** exhibited reversible water absorption as evidenced by IR spectral studies.

The cations present in the cavities of solids are exchangeable by other cations (NH_4^+, Na^+, K^+, etc.) without noticeable change in the framework structures. Thus, when soaked in 2 M aqueous solutions of the electrolyte ECl (E = Na, K, or NH_4) containing the desired cations Na^+, K^+, or NH_4^+ ions) for 24 h with occasional stirring at room temperature, the crystals of **3** and **7** undergo ion exchange accompanied by a decrease in the pH of the electrolyte solutions by 1–1.5 units. Since neither the results of the bond valence sum calculations nor the Fourier difference map indicated the presence of any potentially exchangeable protons associated either with the constituent clusters or bridging groups or within the voids in the structure of **3** and **7**, this drop in pH may be attributed to the ion exchange which may release Li^+ ions from the solid into the solution with accompanying hydrolysis. The presence of any "hidden" acidic groups is, however, less probable but can not be ruled out.

6. COMPOSITE MATERIALS

In our search for the new composite zeolitic materials, we have prepared new hybrid materials incorporating organic ligands in the metal oxide framework (23).

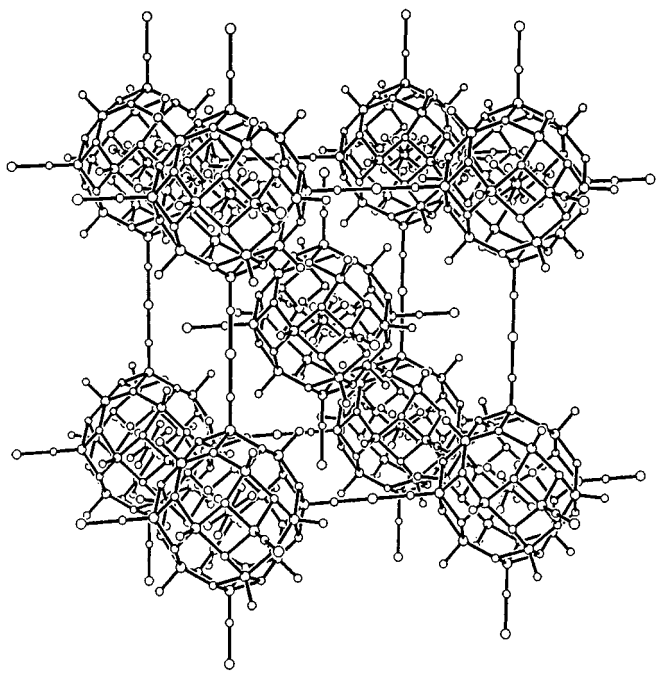

FIG. 5. View of the unit cell showing the extended structure of $[Fe_3(H_2O)_{12}V_{18}O_{42}(XO_4)]\cdot 24H_2O$, **5**, containing arrays of $\{V_{18}O_{42}(XO_4)\}$ interconnected through $\{Fe(H_2O)_4\}$ bridging units. Water molecules have been omitted for clarity.

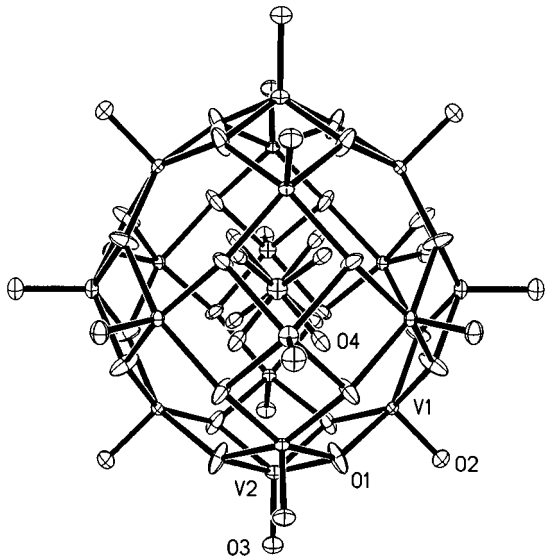

FIG. 6. A view of the $[V_{18}O_{42}(XO_4)]$ cluster in the crystal structure of **5**, showing the atom labeling scheme in the asymmetric unit. The unlabeled central atom, bonded to O4 atoms, represents *X*. Selected bond lengths (Å) and angles (°): **5**: V1–O1 1.948(2), V1–O2 1.587(6), V2–O1 1.942(4), V2–O3 1.636(9), Fe1–O3 2.105(9), V1–O1–V2 98.16(14), V1–O1–V1 138.2(3); **6**: V1–O1 1.923(3), V1–O2 1.590(9), V2–O1 1.954(7), V2–O3 1.652(15), Co1–O3 2.118(14), V1–O1–V2 97.3(2), V1–O1–V1 138.7(5); **7**: V1–O1 1.960(14), V1–O2 1.589(4), V2–O3 1.619(7), Cd1–O3 2.230(6), V1–O1–V2 98.04(11), V1–O1–V1 138.2(2).

$Zn_2(H_2NCH_2CH_2NH_2)_5[\{Zn(H_2NCH_2CH_2NH_2)_2\}_3V_{18}O_{42}(X)]\cdot nH_2O$ is a prototype of the latter type of solids which have been prepared by the hydrothermal reactions of mixtures containing the appropriate vanadate precursors, zinc source (Zn powder or zinc chloride), ethylenediammine (en), and water at 135°C for several hours. Despite some degree of uncertainty in the oxidation states of the vanadium centers and the identity of *X* (likely to Cl and OH), the framework structure of these materials are reasonably resolved ($R \sim 6\%$). The structure (Fig. 8) consists of $\{V_{18}O_{42}(X)\}$ cages interconnected in three dimensions by $\{Zn(H_2NCH_2CH_2NH_2)_2\}$ bridges. The octahedral geometry around the zinc centers in the bridging groups is completed by the two oxo-groups from the two adjacent $\{V_{18}O_{42}(X)\}$ units. The lattice waters and free complex cations $[(en)_2Zn(H_2)NCH_2CH_2N(H_2)Zn(en)_2]^{4+}$ occupy the cavities. The zinc centers in the complex cations are five-coordinate. These are terminally bonded to two chelating (en) ligands and a bridging (en) ligand which links the two zinc centers in the complex. The presence of these bulky cations results in a significant change in the overall structure of the compounds which is manifested into the significantly different connectivity pattern of the constituent $\{V_{18}O_{42}(X)\}$ clusters. Further details of these compounds will be reported in a future publication (23).

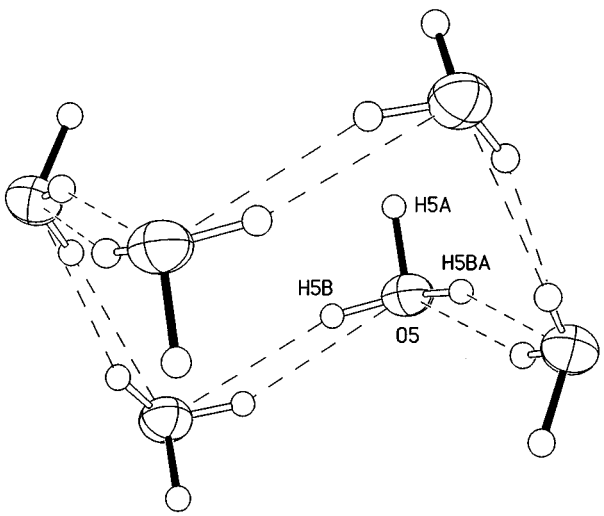

FIG. 7. A view of the lattice water present as $\{(H_2O)_6\}$ clusters in the channels in $Li_6[Cd_3(H_2O)_{12}V_{18}O_{42}(XO_4)]\cdot 24H_2O$ (**7**). The H5B … O5 hydrogen bond distances are 1.94 Å for **7** and 1.87 Å for **3**.

7. CONCLUSION

The syntheses and characterization of the series of framework materials described here represent a step in the direction of the preparation of extended solids composed of well defined oxometalate motifs. In view of the rapidly expanding pool of the well characterized transition metal oxide clusters, this approach has potential to provide access to a variety of new synthetic materials with controllable properties. Given the proven role of polyoxometalates in catalysis (2, 3) and in the development of new oxide supported transition metal catalysts (3f) their application in preparing new surfaces could be valuable. The incorporation of the heterometallic centers (e.g., Mn^{II}, Fe^{II}, Co^{II}, Ni^{II}, Cd^{II}, and Zn^{II}) in these compounds may make it possible to fashion materials that may exhibit properties associated with these sites. In conventional aluminosilicate based zeolites, the reactive transition metal centers are introduced by loading them with the appropriate metal ions or by surface modifications. One of the attributes of the recently developed mesoporous organosilicas is their potential to bind metal ions directly to the framework walls through the ligands (24). The transition metal oxide derived zeolitic materials have such transition metal ions already incorporated into the framework walls. Such materials may find applications in ion exchange, redox catalysis, chemical sensing, and materials science. The incorporation of organic ligands in the metal oxide based solids indicate the possibility of preparing inorganic/organic hybrid materials which may exhibit electronic and optical properties not observed in their pure constituents.

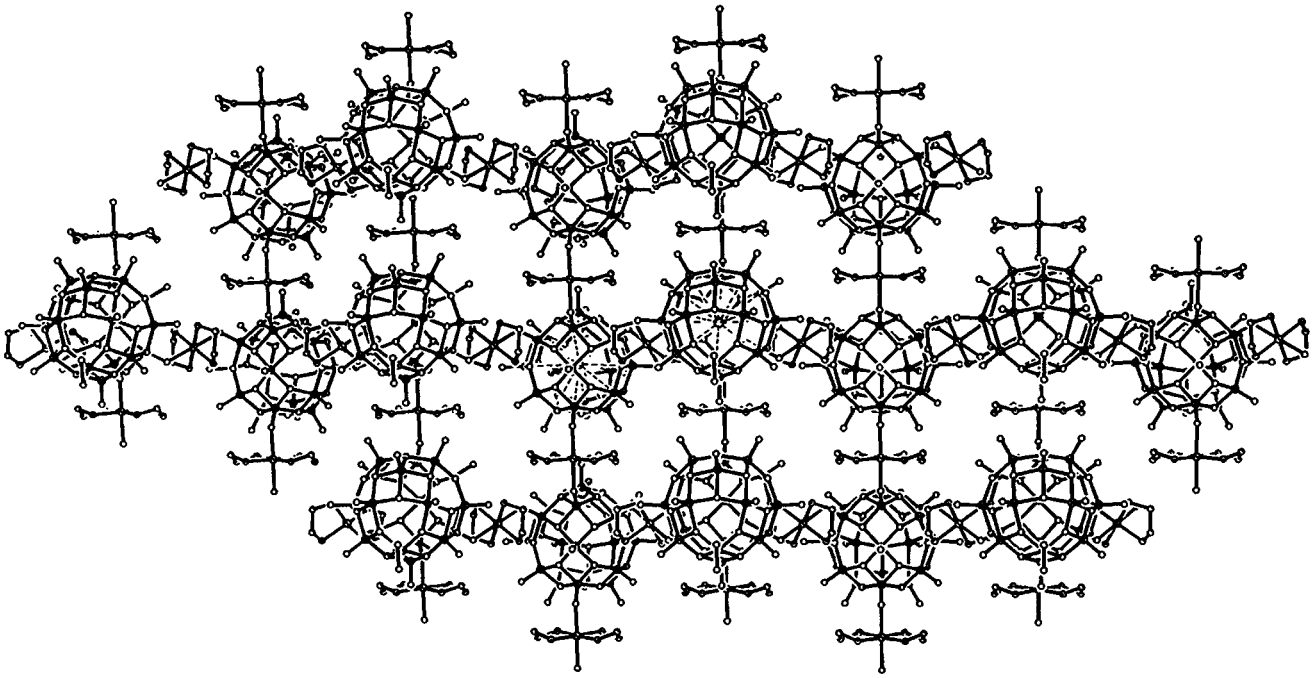

FIG. 8. A view of the extended structure in the crystal structure of $Zn_2(H_2NCH_2CH_2NH_2)_5[\{Zn(H_2NCH_2CH_2NH_2)_2\}_3V_{18}O42(X)]$. Lattice water and cations are not shown.

ACKNOWLEDGMENTS

I express my sincere appreciation to my co-workers, specially to Elizabeth Yohannes, and collaborators, Professor Robert Doedens of the University of California Irvine, and Dr. Douglas Powell of the University of Wisconsin Madison, who have contributed to the results which made possible the preparation of this article.

REFERENCES

1. (a) M. T. Pope, "Heteropoly and Isopoly Oxometalates," Springer, Berlin, 1983; (b) "Polyoxometalates: From Platonic Solids to Anti-Retroviral Activity" (M. T. Pope and A. Müller, Eds.), Kluwer Academic, Dordrecht, 1994; (c) M. T. Pope and A. Müller, *Angew. Chem. Int. Ed. Engl.* **30,** 34 (1991); (d) Some 600 refereed publications and over 120 patents on the chemistry and technology related to polyoxometalates in just one year; for more information, see D. E. Katsoulis, *Chem. Rev.* **98,** 359 (1998), and references. (e) For an up to-date account on some of the most fascinating supermolecular systems, see the following excellent review article: A. Müller, P. Kögerler, and C. Kuhlmann, *J. Chem. Soc. Chem. Commun.* 1347 (1999), and references therein.
2. (a) I. M. Campbell, "Catalysis at Surfaces," Chapman and Hall, London, 1988; (b) H. Kung, "Transition Metal Oxides: Surface Chemistry and Catalysis," Elsevier, New York, 1989; (c) R. K. Grasselli and J. D. Burrington, *Adv. Catal.* **30,** 133 (1981).
3. (a) N. Mizuno and M. Misono, *Chem. Rev.* **98,** 199 (1998); (b) Y. Izumi, K. Urabe, and M. Onaka, "Zeolite, Clay, and Heteropoly Acid in Organic Reactions," VCH, Weinheim, 1992; (c) A. Corma, *Chem. Rev.* **95,** 559 (1995); (d) C. L. Hill, *Coord. Chem. Rev.* **143,** 407 (1995); (e) I. V. Kozhevnikov, *Chem. Rev.* **98**, 171 (1998); (f) M. Pohl, D. K. Lyon, N. Mizuno, K. Nomiya, and R. G. Finke, *Inorg. Chem.* **34,** 1413 (1995), and references therein.
4. W. G. Klemperer, T. A. Marquart, and O. M. Yaghi, *Angew. Chem. Int. Ed. Engl.* **31,** 49 (1992).
5. A. Müller, F. Peters, M. T. Pope, and D. Gatteschi, *Chem. Rev.* **98,** 239 (1998).
6. (a) V. W. Day, W. G. Klemperer, and O. M. Yaghi, *J. Am. Chem. Soc.* **111,** 5959 (1989); (b) A. Müller, E. Krickemeyer, M. Penk, H.-J. Wallberg, and H. Bögge, *Angew. Chem. Int. Ed. Engl.* **26,** 1045 (1987); A. Müller, M. Penk, Ralf Rolfing, E. Krickemeyer, and J. Döring, *Angew. Chem. Int. Ed. Engl.* **29,** 926 (1990).
7. (a) A. Müller, R. Sessoli, E. Krickemeyer, H. Boegge, J. Meyer, D. Gatteschi, L. Pardi, J. Westphal, K. Hovemeier, R. Rohlfing, J. Doring, F. Hellweg, C. Beugholt, and M. Schmidtmann, M. *Inorg. Chem.* **36**, 5239 (1997); (b) G. K. Johnson and E. O. Schlemper, *J. Am. Chem. Soc.* **100**, 3645 (1978).
8. (a) L. Suber, M. Bonamico, and V. Fares, *Inorg. Chem.* **36**, 2030 (1997); (b) A. Müller, M. Penk, E. Krickemeyer, H. Bögge, and H.-J. Wallberg, *Angew. Chem. Int. Ed. Engl.* **27,** 1719 (1988).
9. A. Müller, R. Rolfing, J. Doring, and M. Penk, *Angew. Chem. Int. Ed. Engl.* **30,** 588 (1991).
10. A. Müller, *Nature* **352,** 115 (1991); P. C. H. Mitchell, *Nature* **348,** 15 (1990).
11. E. Coronado and C. J. Gomez-Garcia, *Chem. Rev.* **98,** 273 (1998).
12. (a) V. N. Molchanov, I. V. Tatjanina, and E. A. Torchenkova, *J. Chem. Soc. Chem. Commun.* 93 (1981); (b) T. Yamase and H. Naruke, *J. Chem. Soc. Dalton Trans.* 285 (1991); (c) J. R. Galan-Mascaros, Carlos Gimenez-Saiz, Smail Triki, Carlos Gomez-Garcia, Eugenio Coronado, and Lahcene Ouahab, *Angew. Chem. Int. Ed. Engl.* **34,** 1460 (1995); (d) C. Gimenez-Saiz, J. R. Galan-Mascaros, S. Triki, E. Coronado, and L. Ouahab *Inorg. Chem.* **34,** 524 (1995); (e) Ina Loose, Michael Bösing, Rita Klein, Bernt Krebs, Rolf Schulz, and Bernd Scharbert, *Inorg. Chim. Acta.* **263,** 99 (1997); (f) J. R. D. DeBord, R. C. Haushalter, L. M. Meyer, D. J. Rose, P. J. Zaf,

and J. Zubieta, *Inorg. Chim. Acta* **256,** 165 (1997); (g) M. I. Khan, E. Yohannes, and R. J. Doedens, unpublished results.
13. M. Ishaque Khan, E. Yohannes, and D. Powell, *J. Chem. Soc. Chem. Commun* **23** (1999).
14. M. Ishaque Khan, E. Yohannes, and D. Powell, *Inorg. Chem.* **38,** 212 (1999).
15. M. Ishaque Khan, E. Yohannes, and Robert J. Doedens, *Angew. Chemie. Int. Ed. Engl.* **38,** 1292 (1999).
16. M. Ishaque Khan, E. Yohannes, R. J. Doedens, S. Tabussum, S. Cevik, L. Manno, and D. Powell, *Cryst. Eng.* **2**, 171 (1999).
17. M. Ishaque Khan, S. Tabussum, and C. Zheng, *Polyhedron* (under review).
18. M. Ishaque Khan *et al*., unpublished results.
19. The O_h symmetry refers to the average of the two disordered components. The symmetry, for example, of $\{V_{19}O_{46}\}$ species composed of $\{V_{18}O_{42}\}$ cage encapsulating an ordered $\{VO_4\}$ group will be no higher than T_d.
20. S. R. Batten and R. Robson, *Angew. Chem. Int. Ed. Engl.* **37**, 1460 (1998).
21. (a) For example, the X–O distances (1.538(15) Å for **5** and 1.51(2) Å for **6**) are intermediate between the expected values for SO_4^{2-} and VO_4^{3-}. In the case of **5** (for which the structural results are most precise), the O displacement ellipsoid is elongated along the X–O bond. The displacement parameter of X was higher than expected when it was refined as 100% V and unrealistically low when only S was included. In the final refinement, the displacement parameter of X was fixed at 0.015 $Å^2$ and the relative proportions of V and S were allowed to vary. This model converged to approximately equal proportions of V and S. (b) IR spectra of these compounds exhibit bands attributable to SO_4^{2-} and VO_4^{3-}. Elemental analysis (%S) corresponds to the formulation of **5** and **6**. Our attempts to prepare **5** and **6** without using sulfate did not succeed.
22. I. D. Brown *in* "Structure and Bonding in Crystals" (M. O'Keefe and A. Navrotsky Eds.), p. 1, Academic Press, New York, 1981.
23. M. Ishaque Khan, E. Yohannes, and R. J. Doedens, unpublished results.
24. *Chem. Eng. News*, January 24, 33 (2000).